A R C H I V E S O F M E T A L L U R G Y A N D M A T E R I A L S
Volume 58 2013 Issue 2
DOI: 10.2478/amm-2013-0042

J. ROJEK*, D. LUMELSKYY*, R. PĘCHERSKI*, F. GROSMAN**, M. TKOCZ**, W. CHORZĘPA***

FORMING LIMIT CURVES FOR COMPLEX STRAIN PATHS

GRANICZNE KRZYWE TŁOCZNOŚCI PRZY ZŁOŻONYCH ŚCIEŻKACH ODKSZTAŁCENIA

This paper presents results of experimental studies of forming limit curves (FLC) for sheet forming under complex strain paths. The Nakazima-type formability tests have been performed for the as-received steel blank and for the blank pre-strained by13%. Prestraining leads to abrupt change of strain path in the blank deformation influencing the forming limit curve. The experimental FLC of the pre-strained blank has been compared with the FLC constructed by transformation of the as-received FLC. Quite a good agreement has been found out. The concept of strain-path independent FLCs in polar coordinates has been verified. Two types of the polar diagrams have been considered, the first one with the strain-path angle and effective plastic strain as the polar coordinates, and the second one originally proposed in this work in which the thickness strain has been used instead of the effective plastic strain as one of the polar coordinates. The second transformation based on our own concept has given a better agreement between the transformed FLCs, which allows us to propose this type of polar diagrams as a new strain-path in dependent criterion to predict sheet failure in forming processes.

Keywords: sheet forming, formability, forming limit curve, complex strain-path

W niniejszej pracy przedstawiono doświadczalne badanie granicznych krzywych tłoczności (GKT) w kształtowaniu blach przy zmiennych ścieżkach odkształcenia. Program badań doświadczalnych przedstawionych w pracy obejmował próby tłoczności metodą Nakazimy dla wstępnie wyprężonej blachy rozciągniętej jednoosiowo o 13% oraz takiej samej blachy w stanie niewyprężonym. W wyniku wstępnego wyprężenia w testach otrzymywano silnie nieliniową ścieżkę odkształcenia mającą duży wpływ na GKT. GKT dla blachy wyprężonej porównano z GKT otrzymaną poprzez odpowiednią transformację GKT dla blachy niewyprężonej. Zauważono dość dobrą zgodność między porównywanymi krzywymi.

W pracy przedstawiono i zweryfikowano nową koncepcję odkształceniowych GKT niezależnych od ścieżki odkształcenia. Rozpatrywano dwa rodzaje biegunowych wykresów GKT, w pierwszym przypadku jedną ze współrzędnych biegunowych było efektywne odkształcenie plastyczne, natomiast w drugim przypadku wykorzystano odkształcenie po grubości blachy zamiast efektywnego odkształcenia plastycznego. W drugim przypadku, stanowiącym oryginalną koncepcję zaproponowaną w tej pracy, przetransformowane krzywe GKT dla różnych ścieżek odkształcenia wykazują lepszą zgodność, co pozwoliło nam zaproponować ten rodzaj wykresu biegunowego jako nowe niezależne od ścieżki odkształcenia kryterium tłoczności blach.

1. Introduction

Development of the sheet forming technology requires a better understanding of sheet formability [17,19]. In engineering practice, metal sheet formability is most commonly estimated using the forming limit diagrams (FLD), in which the failure criterion is defined by the forming limit curve (FLC) given in terms of major and minor principal strains. The known drawback of the strain based FLCs is their dependence on strain paths [6]. Forming limit curves are determined for linear or nearly linear strain paths, while real multi-step sheet forming processes are associated with complex deformation paths. Experimental studies of forming under complex strain paths have shown very early that for certain strain paths, combinations of strains above the standard FLC without failure are possible, and conversely, failure may occur with combinations of strains below FLC [13]. Determination of sheet metal formability for changing deformation paths is an issue of great practical importance [12,16].

Forming limit stress diagrams (FLSD) have been proposed as an alternative to the FLD for formability assessment [8,4,2]. Stress-based forming limit curves are less dependent on the strain path effect [15,11], however, the use of FLSD poses some inconviences. Stresses in the deforming sheet cannot be measured directly. They can be determined from the known deformation, however, this requires the use of appropriate constitutive model. Similarly, forming limit stress curves cannot be obtained directly from experiment. Stress based FLC must be calculated from the experimental strain-based FLC or directly from a numerical model [2].

* INSTITUTE OF FUNDAMENTAL TECHNOLOGICAL RESEARCH, POLISH ACADEMY OF SCIENCES PAWIŃSKIEGO 5B, 02-106 WARSAW, POLAND
** SILESIAN UNIVERSITY OF TECHNOLOGY, KRASIŃSKIEGO 8, 40-019 KATOWICE, POLAND
*** KIRCHHOFF POLSKA SP. Z O.O., WOJSKA POLSKIEGO 3, 39-300 MIELEC, POLAND

In view of the above mentioned deficiencies of stress-based forming limit diagrams, it is understandable that strain based forming limit diagrams are still used in practice despite their drawbacks. However, when using strain-based FLCs, one must remember about the strain path effect. Effect of strain path changes on the forming limit curve (FLC) is still the subject of intensive experimental and theoretical work [3,15,1,18]. Possibilities to produce different strain paths experimentally are limited. In many experimental studies, change in deformation path is obtained by employing a two-stage loading procedure, in which the blank is stretched before the formability tests [6,5,7]. Pre-stretching of the material before formability tests leads to abrupt changes in deformation paths influencing the FLC [6,7,14]. Based on the experimental results presented in [5,7] a rule of transformation of the as-received FLC for given pre-strain along the line of constant thickness was proposed by Hosford and Caddell in [10]. In order to overcome the drawback of strain-path dependency of strain-based FLCs a concept of strain-path independent FLCs in polar coordinates has been proposed by Zeng et al [21] and by Stoughton and Yoon [20].

The aim of this study is to investigate experimentally the effect of strain path on the FLC. In particular, the transformation of the as-received FLC for a given pre-strain path proposed in [10], as well as the concept of strain-path independent polar FLCs presented in [21,20] will be verified. In order to improve agreement between experimental FLCs transformed to polar coordinates, a new original idea of polar FLCs will be proposed.

The outline of the paper is as follows. First, experimental procedure is described in Sec. 2. Experimental results for the as-received blank are presented in Sec. 3 in the form of forming limit diagrams. The forming limit curve constructed for the as-received blank is transformed for the initial pre-strain according to the rule presented in [10] in Sec. 4. Results of formability tests for the pre-strained blank are used to determine the FLC for the pre-strained blank. This FLC will be compared to the FLC obtained by the transformation of the as-received FLC. In Sec. 5, transformation of the standard FLC to polar coordinates proposed by Zeng et al [21] and by Stoughton and Yoon [20] will be explained. Following this idea, our experimental FLCs for the as-received and pre-strained blanks will be transformed to the polar coordinates. Finally, a new concept of polar forming limit diagrams will be introduced and verified.

2. Experimental procedure

Nakazima-type formability tests consisting in stretching of the blank over a hemispherical punch have been carried out for the steel grade DC04 1 mm thick. Figure 1 shows the geometry and set-up of the tools. The tests have been performed for the as-received sheet supplied by the manufacturer and for the blank pre-stretched in uniaxial tension conditions by13% along the rolling direction.

Geometry and layout of the specimens on the sheet is shown in Fig. 2. Specimens of different widths have been used, which allowed us to obtain different strain paths. The undercut specimens were oriented in two perpendicular directions.

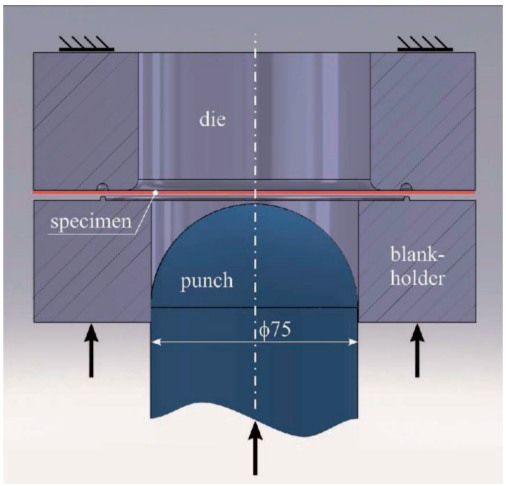

Fig. 1. Formability test set-up

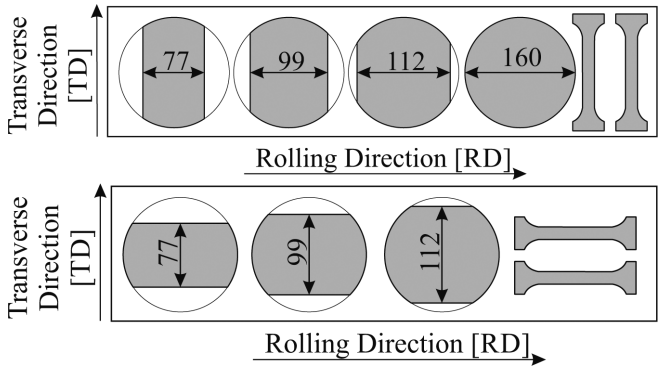

Fig. 2. Geometry and layout of specimens for formability tests

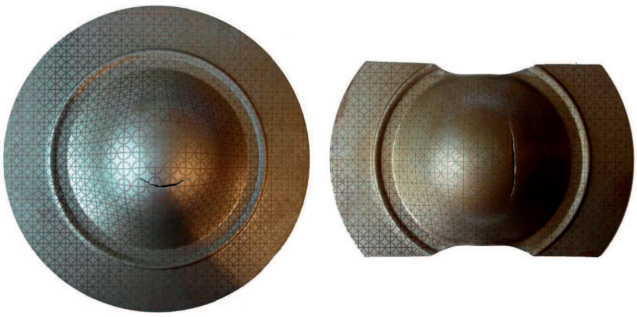

Fig. 3. Selected specimens after formability tests

Half of the specimens cut from the as-received blank were aligned along the rolling direction (RD) and the other half were aligned in the transverse direction (TD). Similarly, the specimens cut from the pre-deformed blank were oriented both parallel and perpendicularly to the rolling and pre-stretching directions. Combination of pre-stretching and subsequent deformation during the formability tests produced complex strain paths leading to localization and fracture. Typical fractured specimens after formability tests are shown in Fig. 3.

The uniaxial tension tests completed the experimental procedure. The tension tests have also been performed for the as-received and pre-strained blanks. The results of the tension tests for the as-received blank and pre-strained blanks are given in Tables 1 and 2, respectively. The specimens have been oriented at 0°, 45° and 90° with respect to the rolling direction in the as-received blank, and at at 0° and 90° with respect

TABLE 1

Results of uniaxial tension tests for the as-received blank

Sample orientation	$R_{p0.2}$ [MPa]	R_m [MPa]	$\frac{R_{p0.2}}{R_m}$	A_{50} [%]	A_{80} [%]	K [MPa]	n for ε_i = 0.02÷0.20	R
0°	175	274	0.64	56.4	47.9	498	0.26	1.7
45°	175	287	0.61	48.6	44.5	506	0.22	1.3
90°	175	282	0.62	52.4	43.4	532	0.26	1.8

TABLE 2

Results of uniaxial tension tests for the blank pre-stretched by 13% along the rolling direction

Sample orientation	$R_{p0.2}$ [MPa]	R_m [MPa]	$\frac{R_{p0.2}}{R_m}$	A_{50} [%]	A_{80} [%]	K [MPa]	n for ε_i = 0.02÷0.10	R
0°	275	285	0.96	42.4	35.8	379	0.08	–
90°	330	330	1	36.7	27.3	379	0.04	–

to the rolling and pre-stretching direction in the pre-strained blank. As it can be expected, the yield strength $R_{p0.2}$ of the pre-strained blank is higher than that of the as-received blank. The ultimate strength R_m of the pre-strained blank determined for the sample aligned in parallel to the pre-stretching direction is similar to the ultimate strength R_m of the as-received material. The stress-strain curves obtained for the pre-strained blank are characterized with a relatively small hardening. Since the range of uniform deformation was very small in the tests performed for the pre-strained blank the Lankford coefficients R have not been determined in these tests.

3. Forming limit diagrams for the as-received blank

Principal strains measured at failure zones of all the specimens after formability and tension tests performed for the as-received blank are plotted in Fig. 4. Separating the points corresponding to safe combinations of strains from those representing fracture the FLC for the as-received material was constructed. This curve is compared with the FLC provided by the steel manufacturer. A good agreement between the two curves can be observed in Fig. 4, which confirms correctness of our experimental procedure and measurements.

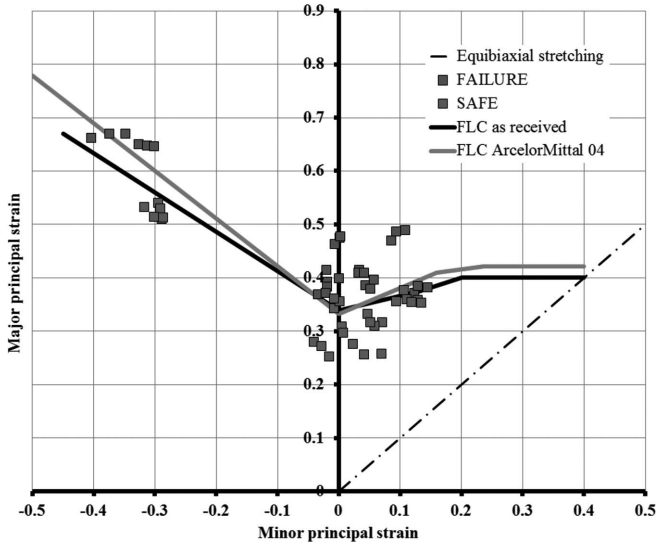

Fig. 4. Forming limit diagram for the as-received blank

The FLD in Fig. 4 gathering all the results does not account for possible influence of planar anisotropy on FLC. If we separate the points on the FLD depending on the alignment of the specimens (Fig. 5) we can obtain two different FLCs, one for the specimens stretched along the rolling direction and the other one corresponding to stretching perpendicularly to the rolling direction. A difference which can be observed between the two FLCs in Fig. 5 reveals the effect of anisotropy on forming limits.

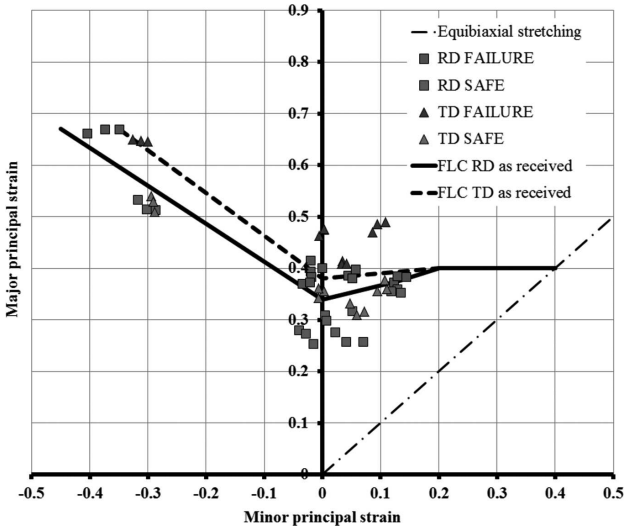

Fig. 5. Forming limit diagram for the as-received blank accounting for anisotropy

Forming limit diagrams accounting for anisotropy can be built taking the rolling direction (RD) as the y-axis and the transverse direction (TD) asthe x-axis. Thus, the FLD shown in Fig. 5 can be transformed into the form presented in Fig. 6. This representation of the FLD is more suitable for different alignment of the specimens and different strain paths than the conventional presentation in terms of major and minor principal strains.

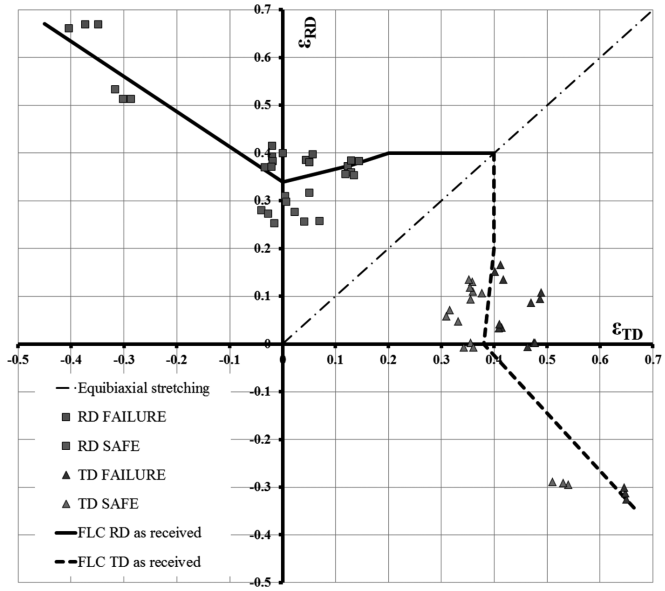

Fig. 6. Forming limit diagram for the as-received blank in material orthotropy axes

4. Forming limit diagrams for the pre-strained blank

Having determined the experimental FLC for the as-received blank we will construct the FLC for the pre-strained blank using the rule proposed by Hosford and Caddell in [10]. According to their suggestion the as received FLC should be shifted along the line $\varepsilon_{TD} + \varepsilon_{RD} = \text{const}$ in such a way that the point corresponding to fracture under plane strain condition will represent the fracture under plane strain path in the transformed FLC. This shift is based on the assumption that the pre-strained sheet breaks at the same thickness strain as the as-received sheet for the plane strain paths.

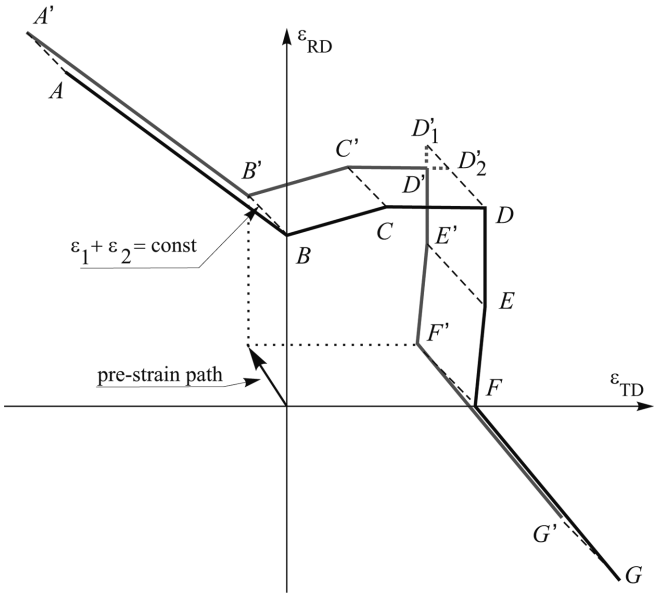

Fig. 7. Construction of the FLC for the blank pre-stretched by 13% according to [10]

Construction of the FLC for the blank prestrained by 13% is shown in Fig. 7. We take the experimental FLC for the as-received blank represented by the line *ABCDEFG*. We draw the vector representing the pre-strain path. From the end of this vector we draw a line parallel to the ε_{RD}-axis representing the plane strain path. Intersection of this line with the line $\varepsilon_{TD} + \varepsilon_{RD} = \text{const}$ passing through the point B is the image B' of the point B in our transformation. Then, translating the points A, C and D by the vector $\overrightarrow{BB'}$ we obtain the line $A'B'C'D'_2$, being the image of the line *ABCD*. Analogously, we perform transformation of the part *DEFG* of the FLC. First, we find the point F' as the intersection of the plane strain path (the plane strain path is parallel to the transverse direction now). and the line of constant thickness passing through the point F. Then, we apply the shift by vector $\overrightarrow{FF'}$ to the points D, E and G. The line $D'_2E'F'G'$ is the image of the line *DEFG*. Combining the limits imposed by the lines $A'B'C'D'_2$ and $D'_2E'F'G'$ we establish the $A'B'C'D'E'F'G'$ as the FLC for the pre-strained blank.

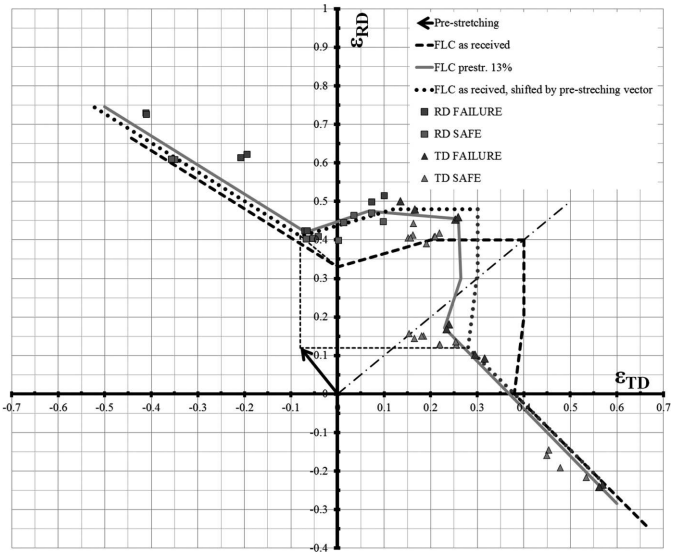

Fig. 8. FLC for the blank pre-stretched by 13% compared to the FLC for the as-received blank

Correctness of the theoretical prediction of the FLC for agiven pre-strain is verified in Fig. 8, in which experimental results of the formability tests for the pre-strained blank are presented. The points corresponding to the local strains measured in experiments are confronted with the as-received FLC and the FLC obtained by shifting the as-received FLC according to the recommendation of Hosford and Caddell [10]. Figure 8 shows that in some cases, fracture appears a little below the shifted FLC, however, the difference is relatively small. This confirms that the shift of the FLC proposed by Hosford and Caddell [10] gives a relatively good approximation here. However, we must remember that this is not always the case, cf. [7].

Experimental results plotted in Fig. 8 allowed us to construct the FLC for the pre-strained blank. As it was observed above, the experimental results are in quite a good agreement with the theoretical prediction, so must the experimental FLC agree with the theoretically constructed FLC. The agreement is better for the part of the FLC obtained from the specimens aligned along the rolling direction (coincident with the pre-strain direction), and it is worse in case of fractures pro-

duced in specimens aligned in the transverse direction (perpendicularly to the pre-strain direction). In the latter case, the change of the strain path is more severe than in the former one.

5. Strain-path independent forming limit diagrams

Strain paths are different for each point in deformed parts so in theory, forming limit curves should be determined for each point depending on its strain path evolution. This is not very practical and therefore possibilities to create strain-path independent FLCs are still searched. A very promising idea of strain-path in dependent FLCs in polar coordinates has been put forward by Zeng et al [21] and recently strongly advocated by Stoughton and Yoon [20]. The authors of this concept are associated with research centers of automotive industry which proves a practical importance of the problem.

Zeng et al [21] derived the path-independent criterion as a limit equivalent plastic strain $\bar{\varepsilon}^p$ depending on the current flow direction β and material properties K, n and R

$$\bar{\varepsilon}^p = f(\beta, K, n, R) \tag{1}$$

where K and n are the Hollomon parameters, R is the average Lankford coefficient, and the current flow direction β is given as

$$\beta = \frac{d\varepsilon_1}{d\varepsilon_2} \tag{2}$$

with ε_1 and ε_1 being the major and minor principal strains. It is convenient to plot the criterion (1) in polar coordinates (r, θ) taking $r = \bar{\varepsilon}^p$ and

$$\theta = \arctan\beta \tag{3}$$

Standard experimental FLCs can be easily converted to the polar FLCs. The transformation of the FLC from the space of principal strains to the polar coordinates is explained in Fig. 9. For an arbitrary point C of the standard FLC we take the angle θ of the strain path as one of the polar coordinates, and the second one is obtained by evaluation of the equivalent plastic strain corresponding to the point C. Assuming the Hill'48 model [9] with normal anisotropy the equivalent plastic strain is given as follows

$$\bar{\varepsilon}^p = \frac{1+R}{2R}\sqrt{\varepsilon_1^2 + \varepsilon_2^2 + \frac{2R}{1+R}\varepsilon_1\varepsilon_2} \tag{4}$$

In this way point C_p in polar coordinates is obtained. Applying this procedure to a number of points defining the FLC in the Cartesian coordinates (Fig. 9(a)) we can obtain the FLC in the polar coordinates (Fig. 9(b)).

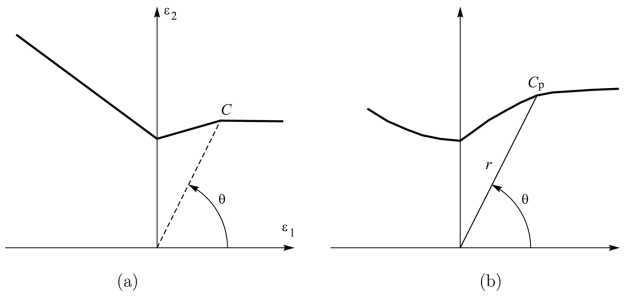

Fig. 9. Transformation of the FLC of the as-received blank from the Cartesian (a) to the polar coordinates (b)

Transformation of the FLC for the complex strain paths is explained in Fig. 10. The transformation procedure is modified by taking the angle defining the strain path at the last stage before fracture as the polar coordinate θ and accumulative evaluation of the equivalent plastic strain

$$\bar{\varepsilon}^p = \sum_{i=1}^{N} \frac{1+R}{2R}\sqrt{\left(\varepsilon_1^{(i)}\right)^2 + \left(\varepsilon_2^{(i)}\right)^2 + \frac{2R}{1+R}\varepsilon_1^{(i)}\varepsilon_2^{(i)}} \tag{5}$$

where N is the number of linear segments in the strain path.

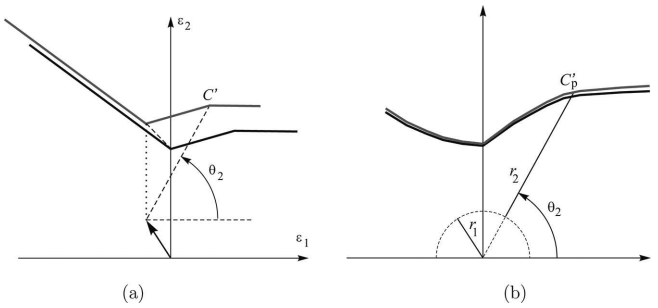

Fig. 10. Transformation of the FLC of the pre-strained blank from the Cartesian (a) to the polar coordinates (b)

Zeng et al [21] and Stoughton and Yoon [20] have applied the transformation presented above to the set of FLCs given by Graf and Hosford [6] and shown that most of the transformed FLCs for different pre-strain coincide with good accuracy in the polar coordinates. This allowed them to take a certain average curve in the polar coordinates as the strain-path independent FLC.

Now, the transformation procedure from the Cartesian to the polar coordinates will be applied to the set of our own experimental FLCs presented in Fig. 11. The set includes the as-received FLC and two FLCs for different pre-strains. The FLCs considered are also presented in Fig. 8. One of the FLCs in Fig. 11 have been obtained by swapping coordinates in one of the FLCs presented in Fig. 8. Applying the transformation described earlier a set of FLCs in the polar coordinates shown in Fig. 12 is obtained. Keeping the angle constant and averaging the radius in the polar diagrams an average FLC is obtained which can be used as the strain-path in dependent FLC.

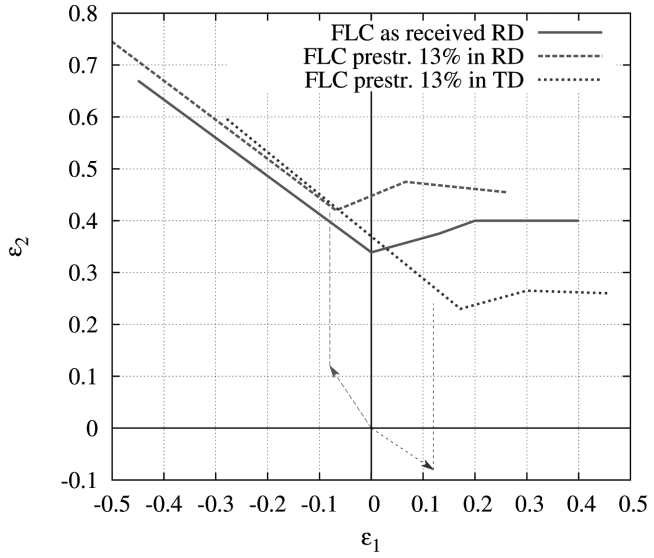

Fig. 11. Set of experimental FLCs in the Cartesian coordinates

Analysing the set of transformed FLCs in the polar coordinates (Fig. 12) we observed a larger discrepancy than we expected. However, such discrepancy can be understood since similar disagreement can be noticed for some cases in [21]. This motivated us to check an alternative transformation to the polar coordinates. Instead of the equivalent plastic strain we propose to take the absolute value of the thickness strain $|\varepsilon_3|$ obtained from the condition of constant volume as

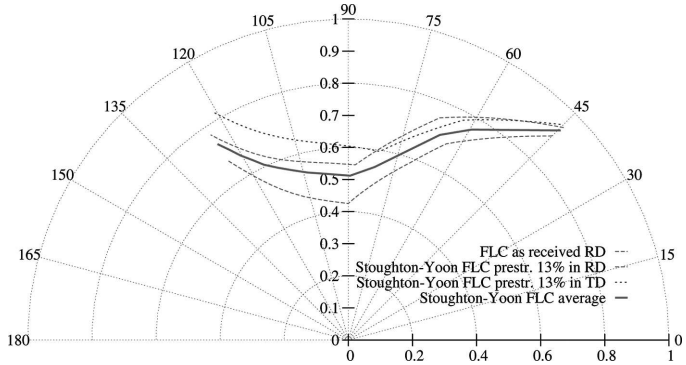

Fig. 12. Set of FLCs after transformation to the polar coordinates according to [21,20]

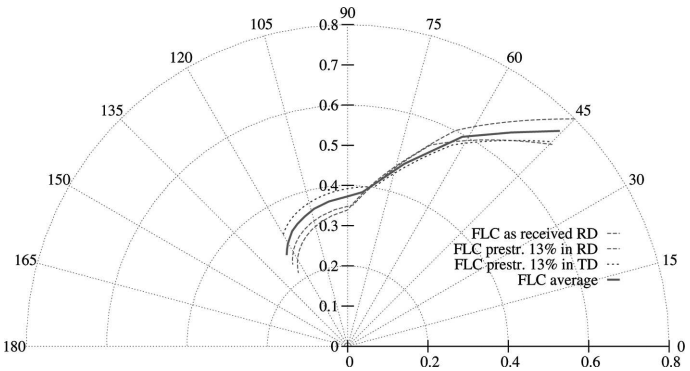

Fig. 13. Set of FLCs after transformation to the polar coordinates according to the new concept

$$\varepsilon_3 = 1 - \varepsilon_1 - \varepsilon_2 \qquad (6)$$

This idea is consistent with the shift of the FLC along the line of constant thickness proposed by Hosford and Caddell in [10], which was discussed above. Applying this transformation to the set of the FLCs shown in Fig. 11 we obtain the polar FLCs plotted in Fig. 13. Much better coincidence of the transformed FLCs can be seen in comparison with the polar FLCs shown in Fig. 12. This indicates that the new concept of the polar FLCs is worth further studies and validation.

6. Conclusions

Formability tests performed for the as-received and pre-stretched blanks confirm the influence of the strain path on the forming limit curves. Standard FLC obtained under linear or nearly linear strain paths cannot be used for complex strain paths. FLCs should be transformed adequately accounting for the strain path. Analysis of the experimental FLCs for the as-received and pre-strained blanks has shown that the transformation of the FLC proposed by Hosford and Caddell [10] gives quite a good prediction of the FLC for the pre-strained blank. Transformation of FLCs from the Cartesian to the polar coordinates introduced by Zeng et al [21] and Stoughton and Yoon [20] can be used to create a strain-path independent forming limit diagrams, however a certain discrepancy is observed among transformed FLCs. The discrepancy was much smaller when a new idea of the polar diagram with the thickness strain as one of the polar coordinates was used. This shows that the polar FLDs according to the idea presented in this paper may be used as failure criterion in sheet forming under complex strain paths, although further validation is necessary.

Acknowledgements

The authors acknowledge funding from: (1) European Regional Development Fund with in the framework of the Innovative Economy Program, project number POIG.01.03.01-14209/09, acronym – NUMPRESS, 2) Ministry of Science and Higher Education through research project N N501 1215 36, (3) National Science Centre through research project No.2311/B/T02/2011/40.

REFERENCES

[1] A. Reyes, O.S. Hopperstad, T. Berstad, O.-G. Lademo, Prediction of necking for two aluminum alloys under non-proportional loading by using an FE-based approach. Int. Journal of Material Forming **1**(4), 211-232 (2008).

[2] T.B. Stoughton, X. Zhu, Review of theoretical models of the strain-based FLD and their relevance to the stress-based FLD. Int. Journal of Plasticity **20**(4), 1463- 1486 (2004).

[3] M.C. Butuc, F. Barlat, J.J. Gracio, A. Barata da Rocha, A new model for FLD predictionbased on advanced constitutive equations. International Journal of Material Forming **3**(3), 191-204 (2009).

[4] M.H. Chen, L. Gao, D.W. Zuo, M. Wang, Application of the forming limit stress diagram to forming limit prediction of the multi-step forming of autopanels. Journal of Materials Processing Technology **187-188**, 173-177 (2007).

[5] A. Grafand, W.F. Hosford, Calculations of forming limit diagrams for changing strain paths. Metallurgical and Materials Transactions A **24**, 2497-2501 (1993).

[6] A. Grafand, W.F. Hosford, Effect of changing strain paths on forming limit diagrams of Al2008-T4. Metallurgical and Materials Transactions A **24**, 2503 (1993).

[7] A. Grafand, W.F. Hosford, The Influence of Strain-Path Changes on Forming Limit Diagrams of A16111T4. International Journal of Mechanical Sciences **36**(10), 897- 910 (1994).

[8] J. Gronostajski, Sheet metal forming-limits for complex strain paths. Journal of Mechanical Working Technology **10**, 349-362 (1984).

[9] R. Hill, A theory of the yielding and plastic flow of anisotropic metals. Proceedings of the Royal Society of London. Series A, Mathematical and Physical Sciences **193** (1033), 281-297 (1948).

[10] W.F. Hosford, R.M. Caddell, Metal Forming: Mechanics and Metallurgy. third edition. Prentice-Hall 2007.

[11] K. Yoshida, T. Kuwabara, Path dependence of the forming limit stresses in a sheet metal. International Journal of Plasticity **23**(4), 361-384 (2007).

[12] M. Karali, Examination of the Strength and Ductility of AA-1050 Material Shaped with the Multi-Stage Deep Drawing Method. Archives of Metallurgy and Materials **56**, 2, 223-230 (2011).

[13] T. Kikuma, K. Nakazima, Aspects of deforming conditions and mechanical properties in the stretch forming limits of sheet metals. Transactions of the Iron and Steel Institute of Japan **11**, 827-830 (1971).

[14] D. Lumelskyy, J. Rojek, R. Pęcherski, F. Grosman, M. Tkocz, Numerical simulation of formability tests of pre-deformed steel blanks. Archives of Civil and Mechanical Engineering **12**, 133-141 (2012).

[15] M. Nurcheshmeh, D.E. Green, Investigation on the strain-path dependency of stress-based forming limit curves. Int. Journal of Material Forming **4**(1), 25-37 (2011).

[16] M. Paćko, M. Dukat, T. Ślebioda, M. Hojny, The analysis of multistage deep drawing of AA5754 aluminum alloy. Archives of Metallurgy and Materials **55**, 4(1033), 1173-1184 (2010).

[17] R. Neugebauer, F. Schieck, S. Polster, A. Mosel, A. Rautenstrauch, J. Schoenherr, N. Pierschel, Press hardening – an innovative and challenging technology. Archives of Civil and Mechanical Engineering **12**, 113-118 (2012).

[18] Q. Situ, M.K. Jain, D.R. Metzger, Determination of forming limit diagrams of sheet materials with a hybrid experimental-numerical approach. Int. Journal of Mechanical Sciences **53**, 9(4), 707-719 (2011).

[19] N. Sene, P. Ballanda, R. Arrieux, Numerical study of the micro-formability of thin metallic materials: virtual micro-forming limit diagrams. Archives of Civil and Mechanical Engineering **11**, 421-435 (2011).

[20] T.B. Stoughton, J.W. Yoon, Path independent forming limits in strain and stress spaces. International Journal of Solids and Structures **49**, 3616-3625 (2012).

[21] D. Zeng, L. Chappuis, Z.C. Xia, X. Zhu, A path independent forming limit criterion for sheet metalforming simulations. SAE Int J Mater. Manuf. **1**, 809-817 (2008).

Received: 15 December 2012.